



Theoretical Study of CH₄ Adsorption and C-H Bond Activation of CH₄ on Metal Ad-atom of M@M (111) (M=Ni, Pd, Pt, Cu, Ag, Au)

Tetsuya Ohkawa^{*}, Kei Kuramoto

Department of Electrical Engineering and Computer Sciences, University of Hyogo, Himeji, Hyogo, Japan

Email address:

univhyogoohkawat@gmail.com (T. Ohkawa)

^{*}Corresponding author

To cite this article:

Tetsuya Ohkawa, Kei Kuramoto. Theoretical Study of CH₄ Adsorption and C-H Bond Activation of CH₄ on Metal Ad-atom of M@M (111) (M=Ni, Pd, Pt, Cu, Ag, Au). *International Journal of Computational and Theoretical Chemistry*. Vol. 4, No. 3, 2016, pp. 21-30.

doi: 10.11648/j.ijctc.20160403.12

Received: November 29, 2016; Accepted: December 8, 2016; Published: January 10, 2017

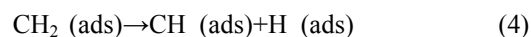
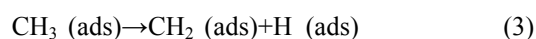
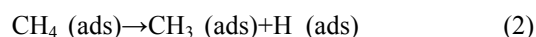
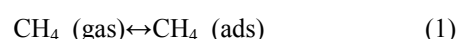
Abstract: We have investigated the CH₄ adsorption and the C-H bond breaking activation on the metal ad-atom of M@M (111) (M=Ni, Pd, Pt, Cu, Ag, Au) and M@M (111)/H (covered by hydrogen atoms) 3 and 1-layer surfaces (4-type surfaces) using spin-polarized Density Functional Theory (DFT). We find that the adsorption energies of methane are related to the d-band center of metal ad-atoms. In particular, the distances between CH₄ and Ni, Pd, and Pt ad-atoms of 4-type surfaces are shortened and the adsorption energies of CH₄ on metal ad-atoms are stronger than the perfect surfaces because the d-band center of metal ad-atoms are close to the Fermi level. Furthermore, we have investigated the activation barrier energies of C-H bond breaking of CH₄ on Ni, Pt, and Ag ad-atoms of 4-type surfaces because Pt ad-atom exhibits stronger adsorption energy of CH₄, Ag ad-atom exhibits weaker ones, and Ni utilizes for the steam reforming reaction. We find that Ni and Pt ad-atoms show lower activation barrier energies, and they are related to the CH₄ adsorption energies as well as the d-band centers.

Keywords: Methane Adsorption, C-H Bond Breaking, Ad-atom, Density Functional Theory

1. Introduction

Methane is a main component of natural gas and is utilized for the steam reforming reaction to produce hydrogen. The methane dissociation reaction is the key process to transform the natural gas into hydrogen. Because of the stability of methane, it is hard to dissociate the C-H bond. In recent years, methane dissociation reaction on metal catalysts has attracted attention [1-9]. Noble metal catalysts show higher activity and stability for this reaction, but very high cost and scarce resources limit those uses. While carbon deposition hinders this reaction and is a severe problem [10-15], Ni-based catalysts become one of the most attractive catalysts in this reaction because of the good catalytic activity and low cost. In fact, the steam reforming reaction on inexpensive Ni catalysts plays an important role in commercial [16, 17]. The C-H bond breaking activation of methane on Ni-based catalysts has attracted much attention in experimentally and theoretically. The methane dissociation reaction is believed to proceed as

follows:



In this reaction scheme, reaction (2) is discussed as the rate-limiting step. In this study, thus, we focus on the adsorption of CH₄ (reaction (1)) and C-H bond breaking reaction of CH₄ (reaction (2)).

In recent years, the dissociative chemisorption of methane on low-index surface of Ni has been extensively studied experimentally and theoretically. Experimentally, for example, molecular beam techniques provide the information in the cleavage of C-H bond such as the activation energy

and the roles of the translational, rotational, and vibrational energies of CH₄. Methane dissociation is activated by both translational and vibrational energy [18-21]. Lee *et al.* studied the activated dissociative chemisorption of CH₄ on Ni(111) surface by molecular beam techniques [22]. They reported that the probability of the dissociative chemisorption of CH₄ increased exponentially with the normal component of the incident molecule's translational energy and with vibrational excitation. Smith *et al.* reported that the vibrational excitation was vibrational excitation of ν_3 (the antisymmetric C-H stretch) activates methane dissociation more efficiently than does translational energy [23]. $2\nu_3$ (the antisymmetric C-H stretch) excitation of methane increases its reactivity by more than 4 orders of magnitude on Ni(111), whereas on Pt(111) the reactivity is lower by 2 orders of magnitude [24].

Theoretical study of quantum chemistry can provide electronic state and atomic level information, giving the theoretical explanation through the computational model. Yang *et al.* studied the dissociative chemisorption of methane at an atom-atom site on a Ni(111) surface by using a many electron embedding theory [25]. They found that the Ni 3d orbitals contributed to the bonding by directly mixing with methane C-H orbitals during the dissociation process. Kratzer *et al.* demonstrated a density functional theory (DFT) study of the first step of CH₄ adsorption on the Ni(111) surface, dissociation into adsorbed CH₃ and H [26]. They revealed that the position of the center of d states was a key quantity for the ability of a surface metal atom to promote the dissociation, and the role of nickel in catalyzing the dissociation of CH₄ was due to its high density of d-states close to the Fermi level. Nave *et al.* used DFT to examine 24 transition states for the dissociation of methane on five different metal surfaces: Ni(111), Ni(100), Pt(111), Pt(100), and Pt(100)-(1×2) [27]. They found that for all five metals, the minimum energy path for dissociation for all five metals was over a top site, with a single (dissociating) H atom pointing toward the surface.

In this study, we focus on the C-H bond breaking activation of methane on the defect of surface. Beebe *et al.* reported that the activation energy of Ni(111), Ni(100), and Ni(110) were 12.6, 6.4, 13.3 kcal/mol, respectively [28]. This result indicated that experimentally methane activation was found to be structure sensitive, with Ni(111) being the least active and Ni(100) and Ni(110) increasingly more active. Bengaard *et al.* studied the effect of steps using a Ni(211) surface, and found the activation energy to be lowered relative to Ni(111) [16]. Abild-Pedersen *et al.* investigated the dissociation of methane on the terraces and steps of a Ni(111) surface by using DFT total energy calculation combined with Ultra High Vacuum (UHV) experiments. They found that the steps exhibited a higher activity than the terrace [29]. Kokaji *et al.* showed that isolated ad-atom of a reactive catalyst on a less reactive surface for dehydrogenation reaction of methane (CH₄→CH₃+H) not only was more active than the perfect or alloy surfaces but also had stronger CH₄ adsorption [30]. Rodríguez-Kessler *et*

al. investigated structural, magnetic, and adsorption property of Ni_n (n=2-16, 21, 55) clusters based on spin polarized DFT, and reported that the CH₄ was adsorbed on the top site of all Ni_n clusters with ranging from -0.17 to -0.47 eV [31]. Yuan *et al.* studied the dehydrogenation processes of CH₄ on the flat Cu(100), Cu ad-atom on Cu(100) surface (Cu@Cu(100)), and Ni@Cu(100) surface via spin polarized DFT approach, and their calculated results showed that the reaction barrier for methane dehydrogenation were remarkably reduced by about 40%-60% with the assistance of the adsorbed Ni atom on the Cu(100) surface, especially for the reaction of CH₄→CH₃+H and CH→C+H [32].

In the present paper, we investigate the CH₄ adsorption and C-H bond activation of CH₄ on Ni@Ni(111), Pd@Pd(111), Pt@Pt(111), Cu@Cu(111), Ag@Ag(111), and Au@Au(111) via spin polarized DFT calculation to evaluate the effect of defect surface such as ad-atom, and the relation between the adsorption energy of CH₄ and the d-band center of metal ad-atom. In addition, we select a few metal ad-atom surfaces and compare the C-H bond activation of CH₄ on metal ad-atoms.

2. Computational Details

We carried out DFT calculations implemented through the PWscf code Quantum Espresso [33]. The exchange and correlation energy functional is treated by using the Perdew-Burke-Ernzerhof (PBE) approximation within the generalized gradient approximation (GGA) [34]. To account for the magnetic moment of nickel, we considered spin polarized electrons. A plain wave basis set with a kinetic energy cutoff of 30 Ry is employed for the valence electrons. A Fermi smearing of 0.01 Ry is utilized to determine electronic occupancies. A sampling of 4×4×1 k-points of the Monkhorst-Pack [35] scheme is used to model the Brillouin zone. Force less than 0.001 eV/Å is used as the criterion for the relaxation convergence. The relaxation of the electronic degrees of freedom is thought to be converged when the energy differences are less than 5×10⁻⁶ eV. A 12 Å vacuum slab is inserted into the direction perpendicular to the surface to separate the neighboring repeated slabs and ensure that the adsorbates and the repeated slab would not interact. The searching for the transition state and geometries of the reaction pathways of the first dissociation reaction of methane (CH₄→CH₃+H) on metal ad-atom surfaces were performed with the climbing-image nudged elastic band (CI-NEB) method [36].

The thickness of the surface models was chosen as a three-layer slab, which is proven reasonable to investigate the mechanism of the adsorption and reaction in previous report [37-39]. The all Ni(111), Pd(111), Pt(111), Cu(111), Ag(111), and Au(111) substrates are modeled by a 1-layer and 3-layer p(2×2) slab containing 4 metal atoms per layer. To investigate the methane adsorption and activity on metal ad-atom, Ni@Ni(111), Pd@Pd(111), Pt@Pt(111), Cu@Cu(111), Ag@Ag(111), and Au@Au(111) are considered by adsorbing one Ni, Pd, Pt, Cu, Ag, and Au atom on the first layer of

Ni(111), Pd(111), Pt(111), Cu(111), Ag(111), and Au(111) substrates, respectively. During the geometry optimization, the bottom one layer is fixed and the other layer and adsorbates are fully relaxed on 3-layer surface system, while surface atoms are fixed and adsorbates are fully relaxed on 1-layer surface system. Here, Zhang *et al.* employed DFT method to comparatively probe into CH₄ dehydrogenation on four types of Cu(111) surface, including the flat Cu(111) surface and the Cu(111) surface with one surface Cu atom substituted by one Rh atom, as well as the Cu(111) surface with one Cu or Rh ad-atom [40]. They found that the differences for the highest barrier between Cu@Cu(111) and Cu(111) surfaces were smaller, the catalytic behaviors of Cu@Cu(111) surface were very close to the flat Cu(111) surface. In this study, we consider two types surface models, that is, 3-layer and 1-layer surface models to check the effect of morphology of surface models. In addition, Abild-Pedersen *et al.* also reported the sulfur and carbon pre-adsorbed Ni surface system [29]. They found that the activation energy barrier for the C-H bond breaking decreased when the d-band was closer to the Fermi level, and the dissociation of methane on sulfur and carbon pre-adsorbed Ni(211) surface were deactivated as compared to clean Ni(211) surface because their d-band centers were down shifted due to sulfur and carbon pre-adsorption. In this study, thus, hydrogen atoms cover metal surface system on the other side of metal ad-atom as a factor to make d-band shift.

The adsorption energy E_{ads} is calculated as follow:

$$E_{ads} = E_{adsorbate/surface} - E_{adsorbate} - E_{surface} \quad (6)$$

where $E_{adsorbate/surface}$ is the total energy of the adsorbate on surface slab model, $E_{adsorbate}$ is the total energy of adsorbate, $E_{surface}$ is the total energy of the surface slab model. The isolated adsorbate models are calculated in a $10 \times 10 \times 20$ space. Here, Yuan *et al.* reported that the calculated zero point energy correction for activation barrier energies of C-H bond dissociation were $0.1 \sim 0.2$ eV [32], which did not change the main conclusion on the relative catalytic activities of the flat Cu(100), Cu@Cu(100), and Ni@Cu(100) surfaces. In this study, thus, we did not calculate the zero point energy

correction because our calculated surface models are similar to their ones.

3. Results and Discussion

3.1. CH₄ Adsorption on Perfect M (Ni, Pd, Pt, Cu, Ag, Au) and M/H 3 and 1-Layer Surfaces

According to the previous theoretical reports, the adsorption energy of CH₄ is extremely small (~ 0.02 eV) [41-43]. Similarly, CH₄ adsorption is reported to be physisorption process on Ni-M (M=Co, Rh, Ir) alloy surfaces [44]. The adsorption energies of CH₄ and the distances of C-H bond length of CH₄ on perfect M(111) (M=Ni, Pd, Pt, Cu, Ag, Au) and M/H(111) 3 and 1-layer surfaces are summarized in Table 1. Our calculated result also shows that the adsorption energies of CH₄ on all M(111) 3-layer surfaces are about $0 \sim -0.04$ eV, which mean physisorption. Although we consider the perfect 1-layer Ni, Pd, Pt, Cu, Ag, Au surface to improve the CH₄ adsorption as compared to the perfect 3-layer surfaces, the adsorption energies of CH₄ are not enhanced for all six M(111) 1-layer surfaces. The calculated adsorption energies of CH₄ on perfect 1-layer Ni, Pd, Pt, Cu, Ag, Au surface are also extremely small (about $0 \sim -0.05$ eV). This result indicates that changing the thickness of metal surface layers has almost no effect for CH₄ adsorption on this perfect metal surfaces system. In addition, we also consider the adsorption of CH₄ on perfect metal surfaces covered by hydrogen atoms to check the effect of covering metal surface on the other side with H atoms. As shown in Table 1, the adsorption energies of CH₄ on M(111) both 3-layer and 1-layer metal surfaces covered by H atoms (M(111)/H) are ranging from about 0 to -0.05 eV. Both Ni(111)/H 3 and 1-layer surfaces show the strongest adsorption energies of -0.048 eV and -0.043 eV, respectively, and Au(111)/H 3-layer and Ag(111)/H 1-layer surfaces show the weakest ones (-0.003 eV and -0.002 eV). This result indicates that the effect of covering metal surface on the other side with H atoms makes no difference on the adsorption of CH₄.

Table 1. The adsorption energies of CH₄ (E_{CH_4}) and the distances of C-H bond length of CH₄ (d_{C-M}) on perfect M(111) (M=Ni, Pd, Pt, Cu, Ag, Au) and M/H 3 and 1-layer surfaces.

Surface		Ni	Pd	Pt	Cu	Ag	Au
3-layer	E_{CH_4} [eV]	-0.048	-0.011	-0.012	-0.006	0.004	-0.003
	d_{C-M} [Å]	4.289	3.778	4.596	4.575	5.345	4.383
3-layer covered by H atom	E_{CH_4} [eV]	-0.049	-0.014	-0.024	-0.009	0.005	-0.003
	d_{C-M} [Å]	4.220	3.626	3.922	4.621	5.547	4.618
1-layer	E_{CH_4} [eV]	-0.043	-0.010	-0.011	-0.009	-0.003	-0.014
	d_{C-M} [Å]	4.327	4.526	4.535	4.527	4.526	4.525
1-layer covered by H atom	E_{CH_4} [eV]	-0.043	-0.012	-0.024	-0.006	-0.002	-0.002
	d_{C-M} [Å]	4.327	4.525	4.518	4.789	4.526	4.524

3.2. CH₄ Adsorption on Metal Ad-atom of M@M (M=Ni, Pd, Pt, Cu, Ag, Au) and M@M/H 3 and 1-Layer Surfaces

We investigate the effect of metal ad-atom for the adsorption of CH₄ on 3-layer surface. The calculated

adsorption energies of CH₄ on metal ad-atom of M@M(111) (M=Ni, Pd, Pt, Cu, Ag, Au) and the distances between C atom of CH₄ and metal ad-atom of M@M(111) are summarized in Table 2. From Table 2, the adsorption energies of CH₄ on metal ad-atom of all M@M(111) surfaces are higher than those on the perfect M(111) 3-layer surfaces.

Although the adsorption energies of CH₄ are in physisorption level (-0.046 ~ -0.235 eV), Ni@Ni(111), Pd@Pd(111), Pt@Pt(111) show twice higher than Cu@Cu(111), Ag@Ag(111), Au@Au(111). This result indicates that the CH₄ prefers to adsorb on the metal ad-atoms rather than the surface metal atoms. Therefore, the dissociation reaction of CH₄ should occur on the metal ad-atom.

Similarly in section 3.1, we consider the adsorption of CH₄ on metal ad-atom of M@M(111) 1-layer surfaces. As compared to M@M(111) 3-layer surfaces, the adsorption energies of CH₄ are strengthened and weakened. As shown in Table 2, the adsorption energies of CH₄ on Pt and Au ad-atoms are strengthened from -0.199 eV to -0.296 eV and from -0.058 eV to -0.144 eV, respectively, and those on Ni ad-atom are weakened from -0.235 eV to -0.190 eV, while those on the other metals (Pd, Cu, Ag) are almost not

changed. In accordance with the adsorption energies of CH₄, the distance of C atom of CH₄ and metal ad-atoms of M@M(111) are changed. This result indicates that the CH₄ also prefers to adsorb on the metal ad-atoms rather than the surface metal atoms. Moreover, we find that the adsorption properties of metal ad-atom on 1-layer metal surface are affected by the thickness of metal surface layer as compared to that on 3-layer metal surface. In order to understand the different CH₄ adsorption properties of metal ad-atom of M@M(111), we investigate the electronic structure of metal ad-atoms before CH₄ adsorption. The local and partial density of states (LDOS) of Pt and Ag ad-atoms of M@M(111) and M@M(111)/H 3 and 1-layer surfaces (4-type surfaces) are presented in Figure 1 as examples, and the d-band center of metal ad-atoms of 4-type surfaces are listed in Table 2.

Table 2. The adsorption energies of CH₄ (E_{CH_4}) and the distances of C-H bond length (d_{C-M}) of CH₄ on metal ad-atom of M@M(111) (M=Ni, Pd, Pt, Cu, Ag, Au) and M@M/H(111) 3 and 1-layer surfaces, and the d-band centers of metal ad-atoms (ϵ_d).

Surface		Ni	Pd	Pt	Cu	Ag	Au
3-layer	E_{CH_4} [eV]	-0.235	-0.193	-0.199	-0.105	-0.046	-0.058
	d_{C-M} [Å]	2.282	2.522	2.479	2.706	3.191	3.074
	ϵ_d [eV]	-1.191	-1.398	-1.893	-2.065	-3.762	-2.684
3-layer covered by H atom	E_{CH_4} [eV]	-0.235	-0.176	-0.245	-0.076	-0.040	-0.085
	d_{C-M} [Å]	2.316	2.512	2.450	2.720	3.250	2.873
	ϵ_d [eV]	-1.296	-1.379	-1.798	-2.212	-3.790	-2.857
1-layer	E_{CH_4} [eV]	-0.190	-0.194	-0.296	-0.154	-0.041	-0.144
	d_{C-M} [Å]	1.688	2.558	2.381	1.800	3.063	2.666
	ϵ_d [eV]	-1.562	-1.288	-1.717	-1.846	-3.818	-2.597
1-layer covered by H atom	E_{CH_4} [eV]	-0.302	-0.325	-0.570	-0.043	-0.016	-0.018
	d_{C-M} [Å]	2.171	2.432	2.330	2.752	2.854	3.623
	ϵ_d [eV]	-1.271	-1.012	-1.340	-1.353	-3.094	-2.446

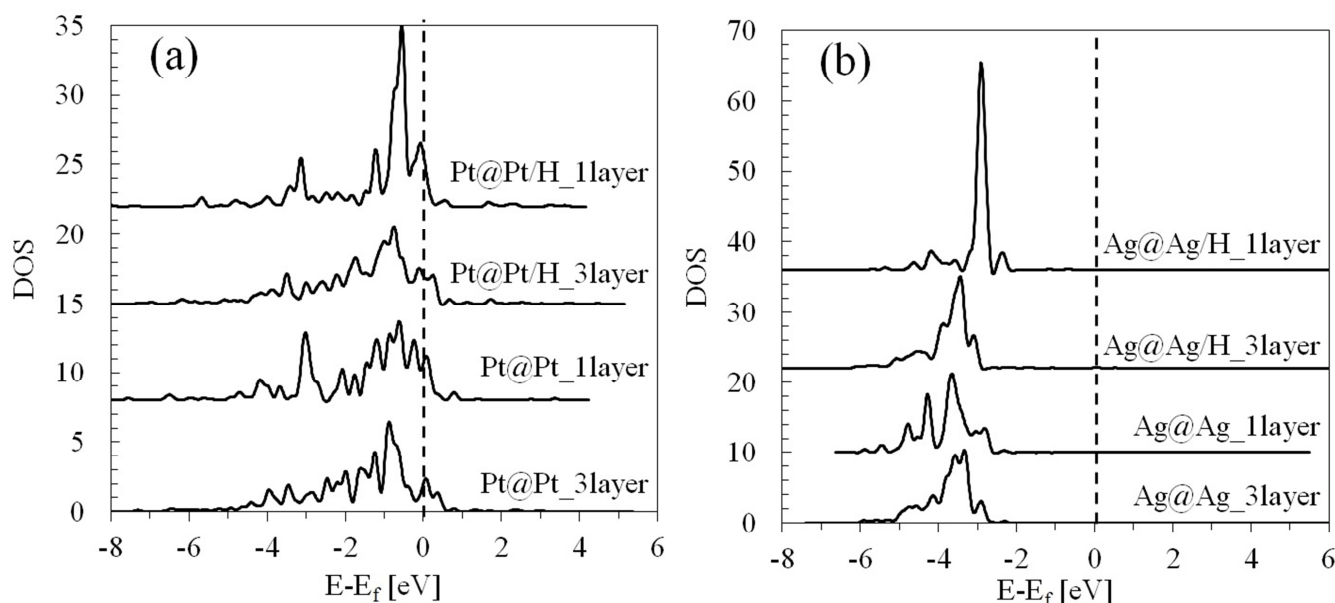


Figure 1. The local and partial density of states (LDOS) of (a) Pt ad-atom of M@M/H(111) and M@M(111) 3 and 1-layer; and (b) Ag ad-atom of M@M/H(111) and M@M(111) 3 and 1-layer surfaces. The dashed line at 0 eV represents the Fermi level.

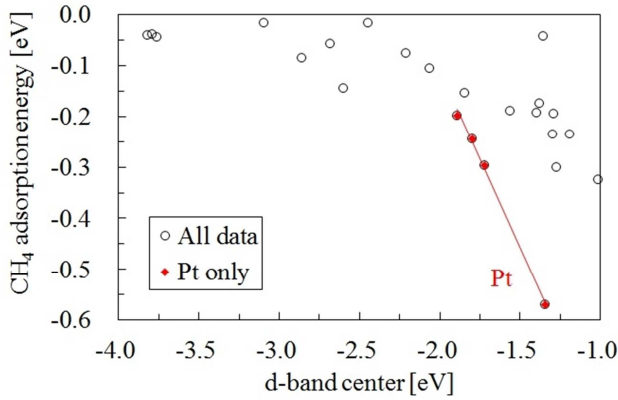


Figure 2. CH₄ adsorption energies on metal ad-atom of M@M(111) (M=Ni, Pd, Pt, Cu, Ag, Au) and M@M/H(111) 3 and 1-layer surfaces as a function of the d-band centers of metal ad-atoms. The Fermi level is set to 0 eV.

As shown in Figure 1, it is clearly shown that the LDOS for Pt ad-atom of 4-type surfaces are larger and closer to the Fermi level than that of Ag ad-atom, and d-band maximum peaks of Pt ad-atom of 4-type surfaces are about -1.0 eV, whereas those of Ag ad-atom of 4-type surfaces are located below about -2.0 eV. Here, it is reported that the position of d-band center correlates with the catalytic activity [29,45,46] as well as the adsorption of adsorbates [47]. As clearly seen from Table 2 and Figure 1, the d-band centers of Pt ad-atom of Pt@Pt(111) 3 and 1-layer and Pt@Pt/H(111) 3 and 1-layer surfaces are -1.398, -1.717, -1.798, and -1.340 eV, respectively, and Ag@Ag(111) 3 and 1-layer and Ag@Ag/H(111) 3 and 1-layer surfaces are -3.762, -3.818, -3.790, and -3.094 eV, respectively. From Table 2, we observe that the d-band centers of all metal ad-atoms of M@M/H(111) 1-layer surface except for Ni are located closest to the Fermi level, while the d-band center of Ni ad-atom of 4-type surfaces are relatively closer to the Fermi level than other metal ad-atom of ones. Figure 2 compares the adsorption energies of CH₄ on metal ad-atom of 4-type surfaces. From Figure 2, the more the d-band centers of metal ad-atoms shift to right, the more the CH₄ adsorption energies become stronger. We find that the adsorption energies of CH₄

correlate with the d-band center of metal ad-atoms on the whole. In particular, the d-band centers of Pt ad-atom of 4-type surfaces are apparently related to CH₄ adsorption energies. This result suggests that changing the thickness of metal ad-atom surface and covering metal surface on the other side with H atoms can make the d-band center of metal ad-atoms shift close to the Fermi level. In particular, metal ad-atoms of M@M 1-layer surfaces are relatively affected by other adsorbed atoms on the other side because of its only one atomic layer.

3.3. CH₄ Adsorption on Metal Ad-atom of M@M (M=Ni, Pd, Pt, Cu, Ag, Au) and M@M/H 3 and 1-Layer Surfaces

As mentioned in section 1, we focus on the adsorption of CH₄ as well as the effect of metal ad-atom, so we investigate only the dissociation reaction of the first step (CH₄→CH₃+H). The other reaction of (CH₃→CH₂+H), (CH₂→CH+H), and (CH→C+H) are not discussed in this study.

Yuan *et al.* studied the dehydrogenation processes of CH₄ on the flat Cu (100), Cu@Cu(100), and Ni@Cu(100) surface via spin polarized DFT approach [32]. They reported that the greatly improved methane dehydrogenation on Ni@Cu(100) arose from the strong Ni-C interaction as compared to Cu@Cu(100) because the Ni-C hybridization region in the transition state of LDOS was deeper and broader as compared to Cu-C hybridization, corresponding to the fact that the Ni-C interaction was stronger than the Cu-C interaction [48]. In addition, the Ni-H interaction was stronger than the Cu-C interaction due to the same reason, and H atom of CH₄ was thus relatively easy to dissociate from the C-H bond of CH₄ on Ni@Cu(100). From this observation, we thought that the C-H bond breaking of CH₄ is also easy to occur when the adsorption energy of CH₄ is stronger. So, we calculate the adsorption energies of CH₃ and dissociated H on M@M(111) (M=Ni, Pd, Pt, Cu, Ag, Au) and M@M/H(111) 3 and 1-layer surfaces to check the relation of adsorption energies between CH₄ and (CH₃ or H), and these results are listed in Table 3.

Table 3. The adsorption energies of CH₃ (E_{CH_3}) and dissociated H (E_H) on M@M(111) (M=Ni, Pd, Pt, Cu, Ag, Au) and M@M/H(111) 3 and 1-layer surfaces.

Surface		Ni	Pd	Pt	Cu	Ag	Au
3-layer	E_{CH_3} [eV]	-2.028	-1.725	-2.143	-1.540	-1.131	-2.031
	E_H [eV]	-1.980	-2.736	-2.334	-1.740	-1.482	-2.447
3-layer covered by H atom	E_{CH_3} [eV]	-1.898	-1.725	-2.240	-1.501	-1.102	-1.896
	E_H [eV]	-1.885	-2.735	-2.509	-2.193	-1.455	-2.323
1-layer	E_{CH_3} [eV]	-1.910	-1.881	-2.380	-1.612	-1.278	-2.060
	E_H [eV]	-1.813	-2.823	-2.201	-2.039	-1.621	-2.478
1-layer covered by H atom	E_{CH_3} [eV]	-1.943	-1.550	-2.487	-1.541	-1.138	-1.762
	E_H [eV]	-2.066	-1.860	-2.644	-1.722	-1.472	-2.181

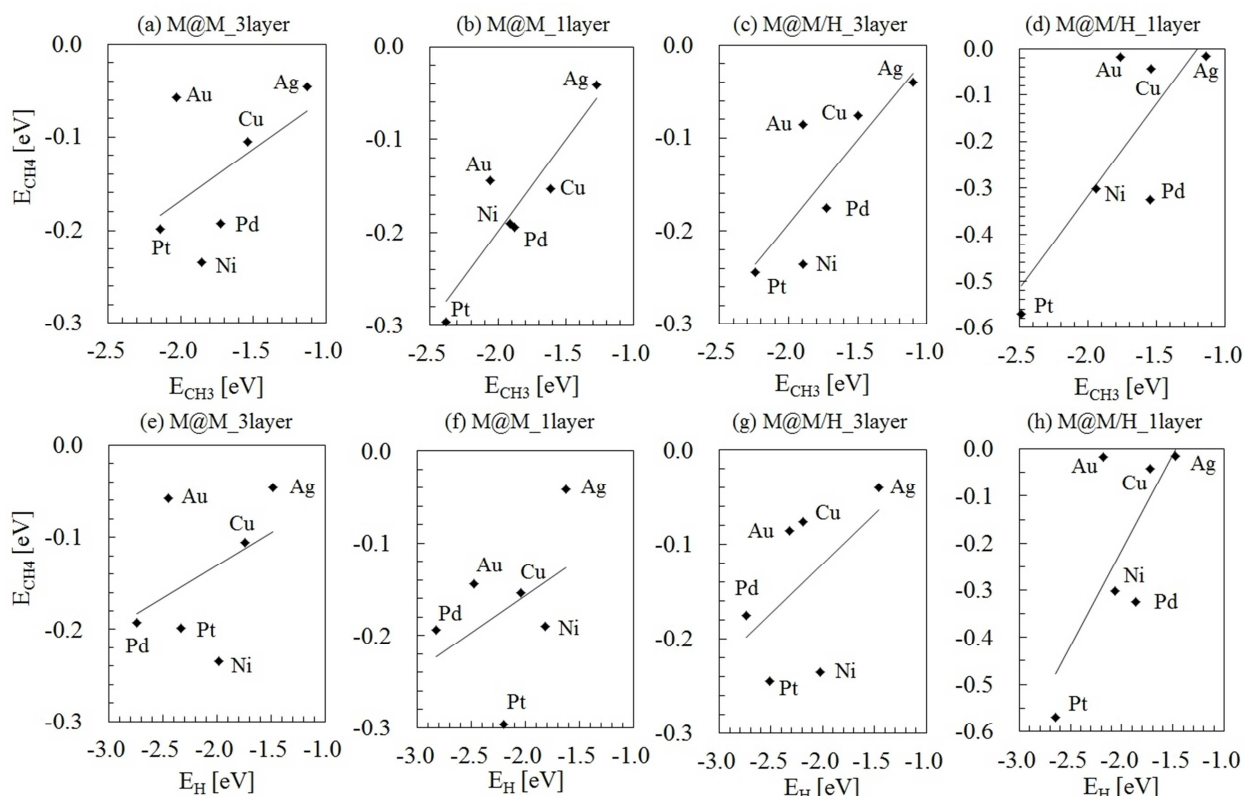


Figure 3. Comparison between the adsorption energies of CH_4 (E_{CH_4}) and E_{CH_3} on metal ad-atom of $M@M(111)$ ($M=Ni, Pd, Pt, Cu, Ag, Au$) and $M@M/H(111)$ 3 and 1-layer surfaces (the upper figures (a)–(d)) and between E_{CH_4} and E_H on metal ad-atom of $M@M(111)$ and $M@M/H(111)$ 3 and 1-layer surfaces (the lower figure (e)–(h)).

From Table 3, the calculated adsorption energies of CH_3 on Ni ad-atom of $M@M(111)$ 3 and 1-layer are stronger than the Cu ad-atom of $M@M(111)$, indicating agreement with the trend studied by previous report that the Ni-C interaction was stronger than the Cu-C interaction [32], whereas the calculated adsorption energies of dissociated H on Ni ad-atoms of $M@M(111)$ 3-layer and $M@M/H(111)$ 1-layer are weaker than Cu ad-atom of those. The first products of CH_4 dissociation reaction are CH_3 molecule and dissociated H atom. Here, we investigate the correlation of the adsorption energy of CH_4 with CH_3 and dissociated H. When the CH_4 adsorption energies correlate with CH_3 or dissociated H adsorption energies, for instance, the graphs of that property draw the linear relation. Figure 3 shows the comparison between the adsorption energies of CH_4 and CH_3 on metal ad-atom of $M@M(111)$ ($M=Ni, Pd, Pt, Cu, Ag, Au$) and $M@M/H(111)$ 3 and 1-layer surfaces, and between the adsorption energies of CH_4 and dissociated H. From Figure 3, the adsorption energies of CH_3 on metal ad-atoms correlate with CH_4 (Figures. 3(a) ~ (d)) in comparison with the adsorption energies of dissociated H (Figures. 3(e) ~ (h)). As can be seen in Figures. 3(e) ~ (h), CH_4 adsorption energies are not related to the dissociated H adsorption energies. On the other hand, as shown in Figures 3(a) ~ (d), there is a relatively correlation between CH_4 and CH_3 adsorption energies (correlation coefficients (R^2) are more than 0.64) except for in the case of $M@M(111)$ 3-layer model (R^2 is 0.25). This result shows that CH_4 adsorption is related to CH_3

adsorption, i.e., metal-C atom interaction, whereas dissociated H adsorption does not affect CH_4 adsorption. Therefore, it is thought that the C-H bond breaking of CH_4 is also affected by the adsorption energies of CH_4 as well as CH_3 .

We estimate the activation barrier energies of C-H bond breaking of CH_4 of the first reaction step ($CH_4 \rightarrow CH_3 + H$) to consider the effect of metal ad-atom, i.e., the effect of enhanced adsorption energies of CH_4 . In this study, we take Ni, Pt, and Ag metal ad-atom of $M@M(111)$ as objects of the dissociation reaction of CH_4 because Pt exhibits stronger adsorption energy of CH_4 , Ag exhibits weaker ones, and Ni utilizes for the steam reforming reaction. Moreover, the adsorption energies of CH_3 on Pt and Ag ad-atom of 4-type surfaces models are the strongest and weakest ones, respectively. The CH_4 dissociation reaction on other metal ad-atom (Pd, Ag, Au) are not treated in this study. The activation barrier energies of C-H bond breaking of CH_4 on Ni, Pt, and Ag ad-atom of $M@M(111)$ and $M@M/H(111)$ 3 and 1-layer surfaces are summarized in Table 4.

Table 4. The activation barrier energies of the C-H bond breaking of CH_4 on metal ad-atom of $M@M(111)$ ($M=Ni, Pt, Ag$) and $M@M/H(111)$ 3 and 1-layer surfaces. All energies are in eV.

Surface type	Ni	Pt	Ag
M@M_3layer	0.787	0.420	2.299
M@M/H_3layer	0.752	0.380	2.333
M@M_1layer	0.866	0.257	2.073
M@M/H_1layer	0.708	0.135	2.432

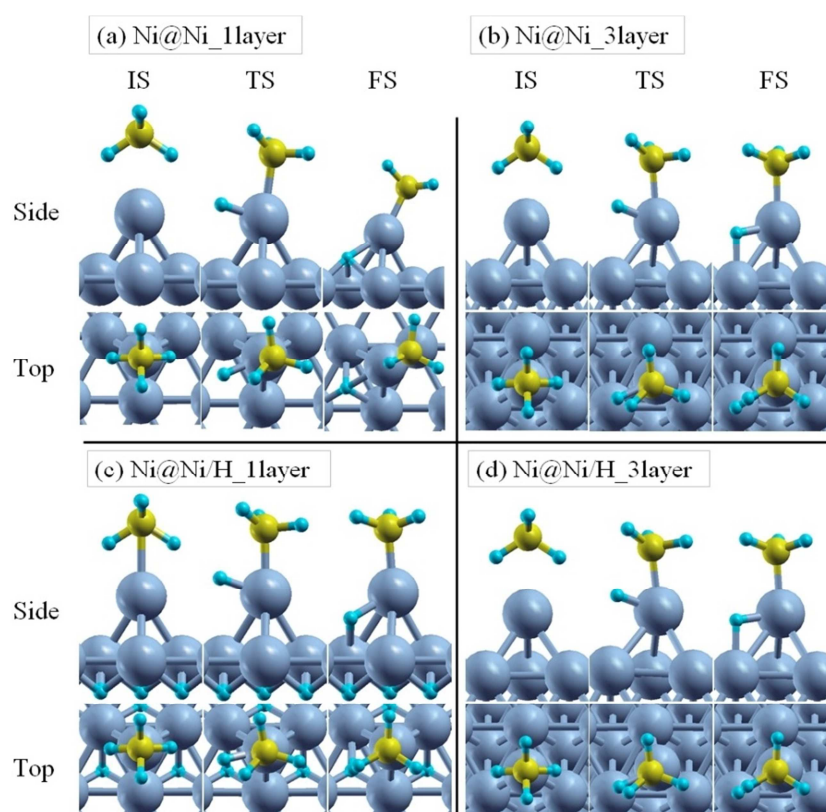


Figure 4. Initial (IS), transition (TS), and final (FS) states of the reaction pathway for the dissociation reaction of CH₄ on Ni ad-atom of Ni@Ni(111) (a) 1 and (b) 3-layer surfaces and Ni@Ni/H(111) (c) 1 and (d) 3-layer surfaces. Upper and lower panel represent the side and top view of surface models, respectively. Yellow, blue, and gray ball denote C, H, and Ni atom, respectively.

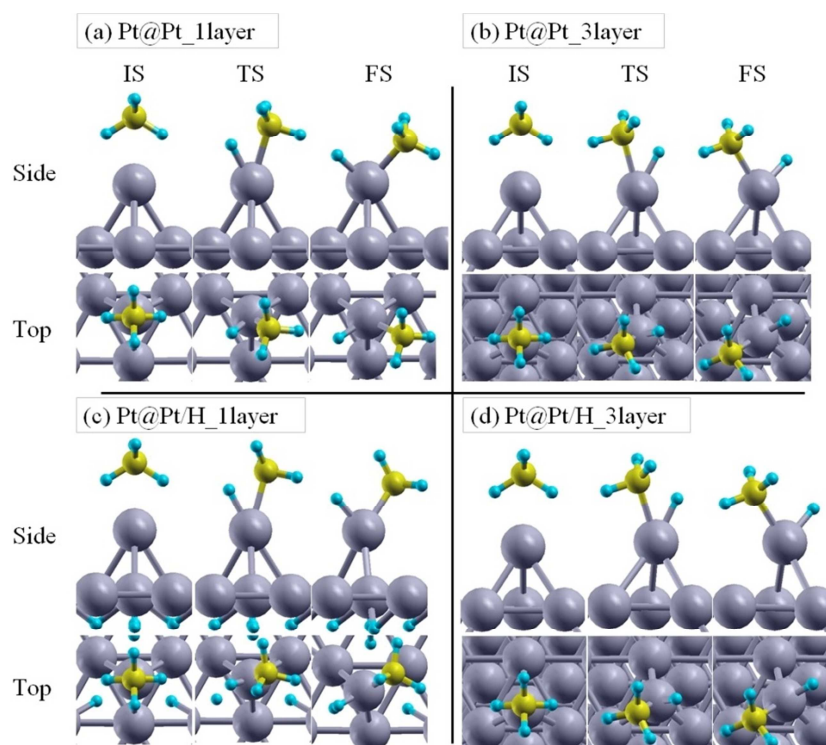


Figure 5. Initial (IS), transition (TS), and final (FS) states of the reaction pathway for the dissociation reaction of CH₄ on Pt ad-atom of Pt@Pt(111) (a) 1 and (b) 3-layer surfaces and Pt@Pt/H(111) (c) 1 and (d) 3-layer surfaces. Upper and lower panel represent the side and top view of surface models, respectively. Yellow, blue, and dark gray ball denote C, H, and Ni atom, respectively.

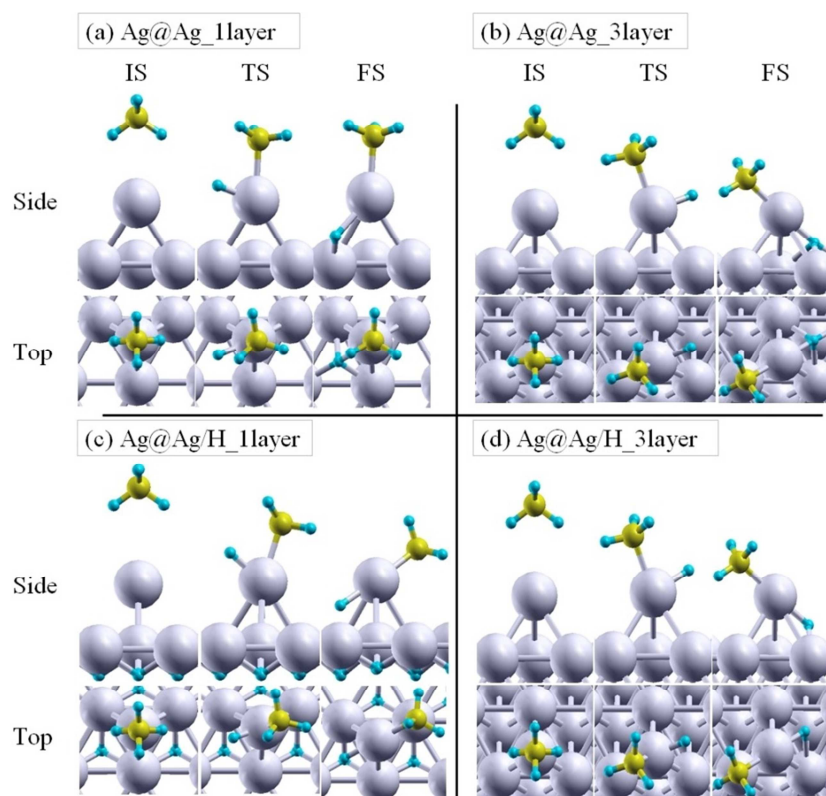


Figure 6. Initial (IS), transition (TS), and final (FS) states of the reaction pathway for the dissociation reaction of CH₄ on Ag ad-atom of Ag@Ag(111) (a) 1 and (b) 3-layer surfaces and Ag@Ag/H(111) (c) 1 and (d) 3-layer surfaces. Upper and lower panel represent the side and top view of surface models, respectively. Yellow, blue, and light gray ball denote C, H, and Ni atom, respectively.

In the case of Ni, CH₄ is adsorbed on Ni ad-atom of Ni@Ni(111) as initial state (IS) configuration which two H atoms of CH₄ are directed to the Ni ad-atom. In the dissociative reaction pathway of CH₄ on Ni ad-atom, as shown in Table 4, H atom is dissociated from CH₄ on Ni ad-atom surfaces with the C-H distance of 1.830 ~ 2.204 Å, and these transition state (TS) geometries are similar to Rh@Cu(111) [30] and (Cu@Cu(100) and Ni@Cu(100)) [32] surfaces. The CH₄ activation barrier energies on Ni ad-atom of 4-type surfaces are 0.708 ~ 0.866 eV which are lower than the perfect Ni(111) surface mentioned previously (1.32 eV [49], 1.12 eV [26], 1.05 eV [29], and 1.04 eV [16]). In the final state (FS) configuration, the dissociated CH₃ molecule is adsorbed on Ni ad-atom, and the dissociated H atom is adsorbed at the bridge site between Ni ad-atom and Ni surface atom of Ni@Ni(111) and Ni/@Ni/H(111) 3-layer surfaces and between Ni ad-atom and Ni three-fold of Ni@Ni(111) and Ni/@Ni/H(111) 1-layer surfaces (see in Figure 4). The configurations of CH₄, CH₃, and dissociated H on Pt and Ag ad-atom of 4-type surfaces are similar to those on Ni ad-atom of ones (see in Figures 5 and 6). In the case of Pt ad-atom, the dissociative reaction of CH₄ on Pt ad-atom show higher activity than Ni and Ag ad-atom. As shown in Table 4, the activation barrier energies of C-H bond breaking of CH₄ on Pt ad-atom of 4-type surfaces range from 0.135 eV to 0.420 eV, which are at least 0.288 eV and 1.653 eV lower as compared to Ni and Ag ad-atom, respectively. It cannot say as a role that changing the thickness of metal surface make C-H bond of CH₄ active because it has not only good

influence on Pt and Ag ad-atom but also bad influence on Ni ad-atom in terms of activation barrier energies. Figure 7 represents the activation energies of C-H bond breaking reaction on Ni, Pt, Ag ad-atoms of 4-type surfaces as a function of the adsorption energies of CH₄ on those ad-atoms (Figure 7(a)) and d-band center of those ad-atoms (Figure 7(b)). From Figure 7(a), the C-H bond activation energies become lower when the adsorption energies of CH₄ is higher in the case of Ni and Pt. It is clearly showed that the activation barrier energies of CH₄ on Ag ad-atom are higher than Ni and Pt ad-atom due to very weak adsorption energies of CH₄. We find that there is a linear correlation between the C-H bond activation barrier energies of CH₄ and the adsorption energies of CH₄, although the activation barrier energies of CH₄ on Ni ad-atom are different from those on Pt ad-atom when CH₄ adsorption energies on both Ni and Pt ad-atom exhibit almost the same values (see in Figure 7(a)). This is observed because the adsorption energies of CH₃ on Ni ad-atom of 4-type surfaces are weaker than the Pd ad-atom of ones (the differences are from 0.115 to 0.624 eV). On the other hand, there is not a linear correlation in the case of Ag. This is due to the weakest adsorption energy of both CH₄ and CH₃. Similarly, as shown in Figure 7(b), the activation energies of the dissociative reaction of CH₄ correlate with the d-band center of Ni and Pt ad-atom. The C-H bond activation energies become lower when the d-band centers of Ni and Pt ad-atoms close to the Fermi level. This trend is in agreement with the previous report [29, 47]. Therefore, it is thought that the adsorbed CH₄ is

easy to be dissociated when its adsorption energies are stronger. This result indicates that the metal ad-atom plays a role to promote the dissociation reaction of CH₄ because

metal ad-atoms can enhance the adsorption energy of CH₄ as compared to the perfect surface and those d-band centers are closer to the Fermi level.

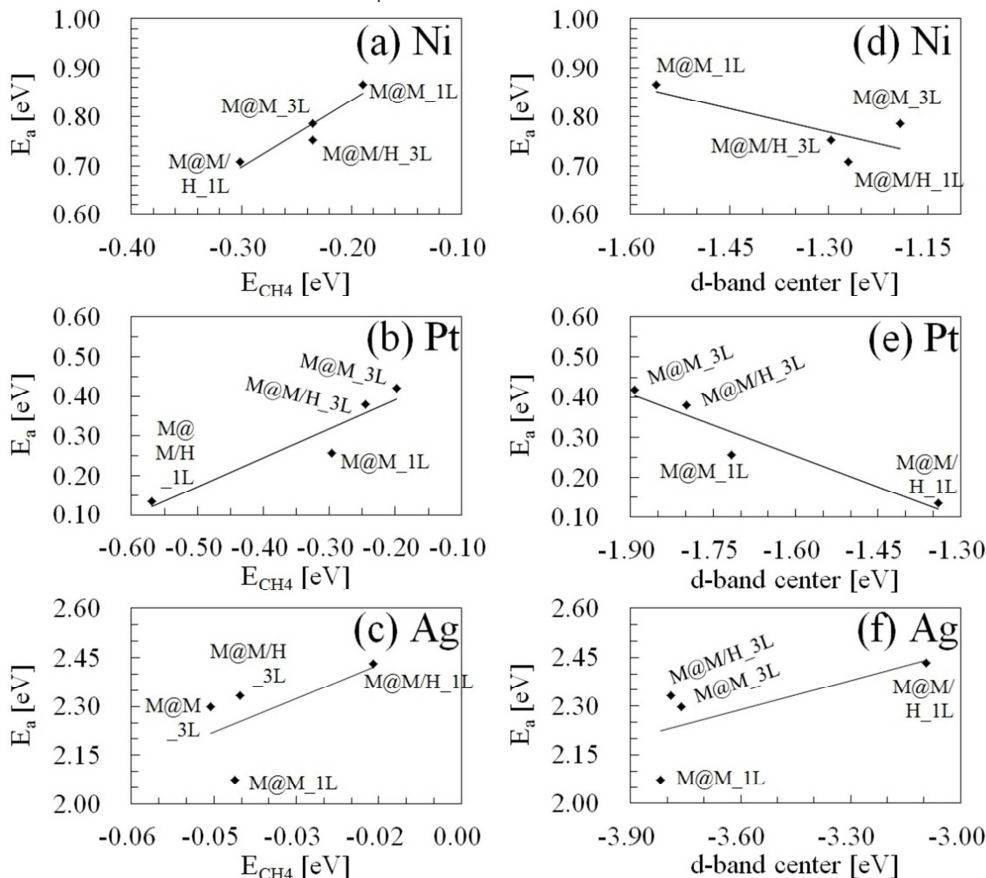


Figure 7. The activation barrier energies of C-H bond breaking of CH₄ (E_a) on M@M(111) (M=Ni, Pt, Ag) and M@M/H(111) 3 and 1-layer surfaces as a function of (a)–(c) the adsorption energies of CH₄ (E_{CH_4}) and (d)–(f) the d-band centers. The Fermi level is set to 0 eV.

4. Conclusion

In summary, we performed spin-polarized DFT calculation to investigate the CH₄ adsorption and dissociation reaction on the metal ad-atom of M@M(111) (M=Ni, Pd, Pt, Cu, Ag, Au) and M@M/H(111) 3 and 1-layer surfaces. Our results indicated that Ni, Pd, and Pt ad-atoms can enhance the adsorption energy of CH₄ as compared to the perfect surfaces, whereas Cu, Ag, and Au ad-atoms showed no apparent change. Changing the thickness of metal surface and covering metal surface on the other side with H atoms can make the d-band center of metal ad-atoms shift close to the Fermi level, and the CH₄ adsorption energies correlate with the d-band center of metal ad-atoms. Moreover, our results showed that the metal ad-atom plays a role to promote the dissociation reaction of CH₄, and C-H bond breaking activation of CH₄ correlates with the adsorption energy of CH₄.

References

- [1] J. R. Rostrup-Nielsen, J. H. B. Hansen, *J. Catal.* 144, 38 (1993).
- [2] M. C. J. Brandford, M. A. Vannice, *Appl. Catal. A Gen.* 142, 97 (1996).
- [3] K. Tomoshige, Y. G. Chen, K. Fujimoto, *J. Catal.* 181, 91 (1999).
- [4] K. Otsuka, S. Kobayashi, S. Takenaka, *Appl. Catal. A Gen.* 190, 261 (2000).
- [5] A. Erdöhelyi, J. Cserényi, F. Solymosi, *J. Catal.* 141, 287 (1993).
- [6] R. Takahashi, S. Sato, T. Sodesawa, M. Kato, S. Takenaka, S. Yoshida, *J. Catal.* 204, 259 (2001).
- [7] O. Tokunaga, Y. Osada, S. Ogasawara, *Fuel* 68, 990 (1989).
- [8] S. Tang, L. Li, J. Lin, H. C. Zeng, K. L. Tan, K. Li, *J. Catal.* 194, 424 (2000).
- [9] A. Malaika, B. Krzyzyska, M. Kozłowski, *Int. J. Hydrogen Energy* 35, 7470 (2010).
- [10] J. M. Ginsburg, J. Pina, T. E. Solh, H. I. de Lasa, *Ind. Eng. Chem. Res.* 44, 4846 (2005).
- [11] J. R. Rostrup-Nielsen, *Catal. Today* 37, 225 (1997).
- [12] V. C. H. Kroll, H. M. Swaan, C. Mirodatos, *J. Catal.* 161, 409 (1996).

- [13] H. M. Swaan, V. C. H. Kroll, G. A. Martin, C. Mirodatos, *Catal. Today* 21, 571 (1994).
- [14] H. F. Abbas, W. M. A. W. Daud, *Int. J. Hydrogen Energy* 35, 141 (2010).
- [15] C. H. Bartholomew, *Appl. Catal. A Gen.* 212, 17 (2001).
- [16] H. S. Bengaard, J. K. Nørskov, J. Sehested, B. S. Clausen, L. P. Nielsen, A. M. Molenbroek, and J. R. Rostrup-Nielsen, *J. Catal.* 209, 365 (2002).
- [17] J. R. Rostrup-Nielsen, Springer, Berlin (1984) (editor: J. R. Anderson, M. Boudart).
- [18] C. T. Rettner, H. E. Pfnur, and D. J. Auerbach, *Phys. Rev. Lett.* 54, 2716 (1985).
- [19] C. T. Rettner, H. E. Pfnur, and D. J. Auerbach, *J. Chem. Phys.* 84, 4163 (1986).
- [20] P. M. Holmblad, J. Wambach and I. Chorkendorff, *J. Chem. Phys.* 102, 8255 (1995).
- [21] L. B. F. Juurlink, P. R. McCabe, R. R. Smith, C. L. DiCologero, and A. L. Utz, *Phys. Rev. Lett.* 83, 868 (1999).
- [22] M. B. Lee, Q. Y. Yang, and S. T. Ceyer, *J. Chem. Phys.* 87, 2724 (1987).
- [23] R. R. Smith, D. R. Killelea, D. F. DelSesto, and A. L. Utz, *Science*, 304, 992 (2004).
- [24] R. Bisson, M. Sacchi, T. T. Dang, B. Yoder, P. Maroni, and R. D. Beck, *J. Phys. Chem. A*, 111, 12679 (2007).
- [25] H. Yang and J. L. Whitten, *J. Chem. Phys.* 96, 5529 (1992).
- [26] P. Kratzer, B. Hammer, and J. K. Nørskov, *J. Chem. Phys.* 105, 5595 (1996).
- [27] S. Nave, A. K. Tiwari, and B. Jackson, *J. Chem. Phys.* 132, 054705 (2010).
- [28] T. P. Beebe Jr., D. W. Goodman, B. D. Kay, and J. T. Yates Jr., *J. Chem. Phys.* 87, 2305 (1987).
- [29] F. Abild-Pedersen, O. Lytken, J. Engbæk, G. Nielsen, I. Chorkendorff, and J. K. Nørskov, *Surf. Sci.* 590, 127 (2005).
- [30] A. Kokaji, N. Bonini, S. de Gironcoli, C. Sbraccia, G. Fratesi, and S. Baroni, *J. Am. Chem. Soc.* 128, 12448 (2006).
- [31] P. L. Rodríguez-Kessler and A. R. Rodríguez-Domínguez, *J. Phys. Chem. C* 119, 12378 (2015).
- [32] S. Yuan, L. Meng, and J. Wang, *J. Phys. Chem. C* 117, 14796 (2013).
- [33] P. Giannozzi, S. Baroni, N. Bonini, M. Calandra, R. Car, C. Cavazzoni, D. Ceresoli, G. L. Chiarotti, M. Cococcioni, I. Dabo, A. Dal Corso, S. Fabris, G. Fratesi, S. de Gironcoli, R. Gebauer, U. Gerstmann, C. Gougoussis, A. Kokalj, M. Lazzeri, L. Martin-Samos, N. Marzari, F. Mauri, R. Mazzarello, S. Paolini, A. Pasquarello, L. Paulatto, C. Sbraccia, S. Scandolo, G. Sclauzero, A. P. Seitsonen, A. Smogunov, P. Umari, R. M. Wentzcovitch, *J. Phys.: Condens. Matter*, 21, 395502 (2009).
- [34] J. P. Perdew, K. Burke, and M. Ernzerhof, *Phys. Rev. Lett.* 77, 3865 (1996).
- [35] H. J. Monkhorst and J. D. Pack, *Phys. Rev. B* 13, 5188 (1976).
- [36] G. Henkelman, B. P. Uberuaga, and H. Jónsson, *J. Chem. Phys.* 113, 9901 (2000).
- [37] V. Shah, T. Li, K. L. Baumert, H. Cheng, and D. S. Sholl, *Surf. Sci.* 527, 217-227 (2003).
- [38] S. G. Wang, X. Y. Liao, J. Hu, D. B. Cao, Y. W. Li, J. Wang, and H. Jiao, *Surf. Sci.* 601, 1271 (2007).
- [39] H. Liu, R. Zhang, R. Yan, B. Wang, and K. Xie, *Appl. Surf. Sci.* 257, 8955 (2011).
- [40] R. Zhang, T. Duan, L. Ling, and B. Wang, *Appl. Surf. Sci.* 341, 100 (2015).
- [41] S. G. Wang, D. B. Cao, Y. W. Li, J. G. Wang, and H. J. Jiao, *J. Phys. Chem. B* 110, 9976 (2006).
- [42] G. Gajewski and C. W. Pao, *J. Chem. Phys.* 135, 064707 (2011).
- [43] K. Li, C. He, M. Jiao, Y. Wang, and Z. Wu, *CARBON*, 74, 255 (2014).
- [44] K. Li, M. Jiao, Y. Wang, and Z. Wu, *Surf. Sci.* 617, 149 (2013).
- [45] B. Hammer and J. K. Nørskov, *Surf. Sci.* 343, 211 (1995).
- [46] B. Hammer, *Top. Catal.* 37, 3 (2006).
- [47] V. Pallassana and M. Neurock, *J. Catal.* 191, 301 (2000).
- [48] J. Ding, Z. Qiao, W. Feng, Y. Yao, and Q. Niu, *Phys. Rev. B* 84, 195444 (2011).
- [49] R. M. Watwe, H. S. Bengaard, J. R. Rostrup-Nielsen, J. A. Dumesic, and J. K. Nørskov, *J. Catal.* 189, 16 (2000).